



Structural characteristics and connection mechanism of gold-catalyzed bridging silicon nanowires

S. Sharma^{a,*}, T.I. Kamins^a, M.S. Islam^a, R. Stanley Williams^a, A.F. Marshall^b

^a*Hewlett-Packard Laboratories, Quantum Science Research, 1501 Page Mill Road, M/S 1123, Palo Alto, CA 94304, USA*

^b*Geballe Laboratory for Advanced Materials, Stanford University, Stanford, CA 94305, USA*

Received 22 October 2004; received in revised form 8 March 2005; accepted 7 April 2005

Available online 24 May 2005

Communicated by J.M. Redwing

Abstract

Lateral, single-crystalline silicon nanowires were synthesized using chemical vapor deposition catalyzed by gold nanoparticles deposited on one of the vertical $\{111\}$ sidewalls of trenches etched in Si(011) substrates. Upon encountering the opposing sidewalls of the trenches, the lateral nanowires formed a mechanically strong connection. The bridging connection at the opposing sidewall was observed using high-resolution transmission electron microscopy (TEM) to be epitaxial and unstrained silicon-to-silicon. Using energy-dispersive X-ray spectroscopy in TEM, gold could not be detected at the interface region where the nanowires formed a connection with the opposing sidewall silicon deposit but was detected on the surface adjacent to the impingement region. We postulate that a silicon-to-silicon connection is formed as the gold–silicon liquid eutectic is forced out of the region between the growing nanowire and the opposing sidewall.

© 2005 Elsevier B.V. All rights reserved.

PACS: 81.05.Y; 81.15.G; 81.20.K

Keywords: A1. Bridging; A1. Nanowires; A3. Chemical vapor deposition; B3. Sensors

1. Introduction

Chemically synthesized semiconductor nanowires are expected to be of interest for a variety

of electronic, optical, and optoelectronic device applications [1,2]. Nanowires, because of their high surface-to-volume ratios are also interesting for sensing applications [3]. Semiconductor nanowires have been synthesized using a variety of techniques [4–7]. However, in order to realize novel sensors using nanowires, these nanostructures must be integrated within a device capable of

*Corresponding author. Tel.: +1 650 236 4031;

fax: +1 650 236 9885

E-mail address: Shashank@hp.com (S. Sharma).

measuring a transducible property, such as electrical conductance. In order to integrate semiconductor nanowires into a device structure, the nanowires should be self-assembled in a massively parallel manner.

Nanometer-scale titanium-silicide islands and Au–Si eutectic droplets have been shown to catalyze the growth of silicon in one dimension to form free-standing nanowires by chemical vapor deposition (CVD) [4,5]. Under suitable experimental conditions, the nanoparticles catalyze the decomposition of a silicon-containing gas at rates orders of magnitude higher than the uncatalyzed, “normal” silicon deposition rate. The resulting silicon atoms diffuse through or around the catalyst nanoparticle and attach at the nanoparticle–silicon interface to propagate one-dimensional growth. The nanowires typically grow epitaxially along the $\langle 111 \rangle$ crystallographic directions, therefore, perpendicular to $\{111\}$ -oriented silicon surfaces.

Recently, we demonstrated lateral growth of gold- and titanium-catalyzed silicon nanowires from a vertical $\{111\}$ sidewall of a trench on a (011)-oriented silicon wafer [8]. Upon impinging on the other sidewall, the nanowires attach to this “opposing” sidewall, thus bridging across the trench and making strong mechanical connection. Bridging nanowires are potentially valuable as elements of electronic devices, such as sensors, since the electrical contacts are formed in-situ by self-assembly. In order to use bridging nanowires in an electronic device, the vertical surfaces bridged by the nanowires can be electrically isolated (on a silicon-on-insulator substrate [9], for example). One of the electrical connections is formed at the base end of the nanowire, while the other connection is formed when the nanowire impinges on the opposing sidewall. The nature of the connection at the impinging end will partially determine the electrical and mechanical behavior of the electronic device, and thus should be investigated in detail. In this paper, we report results of a TEM investigation of the structural characteristics of the bridging Au-catalyzed silicon nanowires, especially the connection to the opposing sidewall. Based on our TEM observations, we also suggest a possible mechanism by which the nanowires attach at the opposing sidewall.

2. Experimental procedure

The nanowires were grown by CVD in a lamp-heated, single-wafer, cool-walled CVD reactor, in which the samples are supported by a SiC-coated graphite plate of moderate thermal mass. The nanowires discussed in this paper were synthesized on an approximately 1"-square piece of a p-type (boron, 4–8 Ω cm) (110)-oriented Si wafer. The photolithography process used to fabricate trenches with vertical sidewalls is discussed in Ref. [8]. After forming the vertical $\{111\}$ surfaces, cleaning the substrate and removing the native oxide with dilute HF, a thin (typically, <1 nm) gold film was deposited by electron-beam evaporation onto the vertical $\{111\}$ surfaces of the etched trenches. The sample was held at an angle of 45° from the normal to deposit the catalyst on only one sidewall of the trenches so that the wires would grow preferentially from one sidewall. The Au-coated substrate was transferred through air to the CVD reactor, where it was annealed in hydrogen ambient (3 slm H₂) for 5 min at 95 Torr at 670 °C. Annealing in hydrogen ambient resulted in nanometer scale particles of gold–silicon alloy. Following annealing, the substrate was exposed to a mixture of 15 sccm SiH₄, 15 sccm HCl, and 3 slm H₂ for 30 min at 10 Torr total pressure and 680 °C to produce a dense array of bridging nanowires. Under these growth conditions, the axial growth rate of the nanowires is 400 nm/min. Although the annealing temperature was significantly higher than the gold–silicon molten eutectic formation temperature, exposure of the annealed gold-coated silicon wafers to a gas mixture containing SiH₄, HCl, and H₂ was necessary to commence nanowire growth.

The samples for cross-sectional TEM investigation were prepared using a Ga⁺ beam in a FEI Strata DB235 focused ion beam (FIB) mill. A cleaved wafer piece was first dipped in M-bond 610 epoxy to provide protection for the nanowires. Pt was then deposited by ion beam deposition to mark the locations of interest. A standard FIB lift-out section was then prepared [10,11]. The TEM investigation was performed using a Philips CM20 microscope (200 keV acceleration voltage) equipped with energy-dispersive X-ray spectroscopy (EDAX, Inc.).

3. Results and discussion

Fig. 1 shows the typical morphology of gold-catalyzed, bridging silicon nanowires synthesized under the experimental conditions described above. Nanowires with diameters ranging from 60 to 200 nm were grown across trenches of varying widths. As shown in the inset in Fig. 1, typically a disc-like deposit was observed at the impinging end. As we reported previously [8], nanowires form mechanically strong connection at the impinging end. The nature of the connection of the nanowires at the impinging end will govern the applicability of the bridged nanowires in devices that require electrical transport.

Fig. 2(a) shows a bright field TEM image of a bridging silicon nanowire near its base. The dark streaks seen in the image are bend contours, rather than line defects, as confirmed by tilting the samples, which caused the bend contours to appear in different regions of the nanowire. The inset in Fig. 2(a) shows a convergent-beam

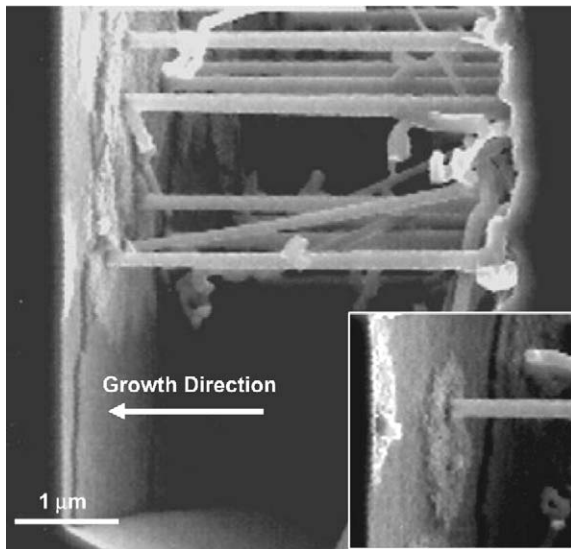
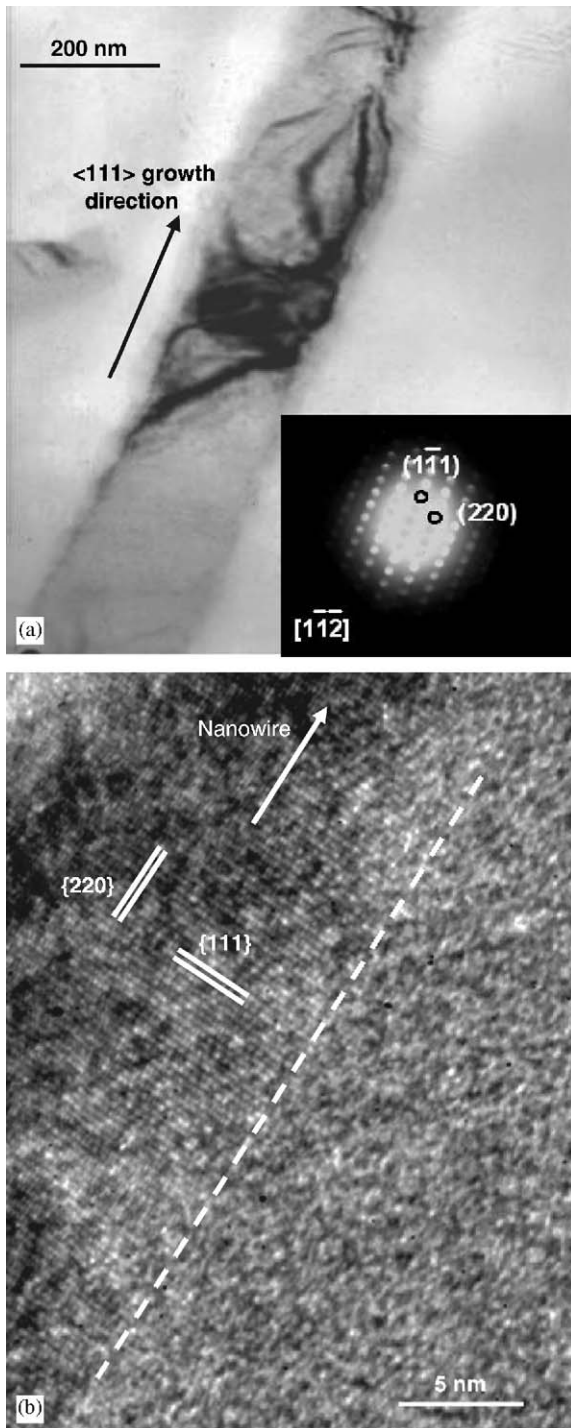


Fig. 1. Representative cross-sectional scanning electron micrograph of gold-catalyzed silicon nanowires bridged between two vertical sidewalls of a 5 μm wide trench. The inset shows the impinging end of a bridging nanowire and the disc-like deposit formed on the “opposing” sidewall. The nanowires were grown at 680 °C for 30 min at 10 Torr using 15 sccm SiH₄, 15 sccm HCl, and 3 slm H₂.

electron diffraction (CBED) pattern taken along the $[1\bar{1}\bar{2}]$ zone axis. Fig. 2(b) shows a high-resolution TEM (HRTEM) image along a portion of a bridging silicon nanowire. The lattice spacing matched the d-spacing of the $\{111\}$ silicon planes. Thus, CBED and HRTEM confirmed the nanowires to be single-crystalline and the growth direction to be along $\langle 111 \rangle$.

Fig. 3(a) shows a bright-field TEM image of the impinging-end region of a bridging silicon nanowire. The bridging nanowire cracked near the impinging-end sidewall during the TEM sample preparation, but the region of interest remained intact for TEM characterization. The broken portion of the nanowire and some other regions of the sample were also amorphized during the TEM sample preparation. The different regions of the impinging-end sidewall have been labeled A through J, and the structural characteristics of each of these regions will be discussed below.

Fig. 3(b) shows a HRTEM image of region A, the interface region between the uncatalyzed silicon deposit that forms at the same time as the nanowire grows and the impinging-end sidewall. Uncatalyzed deposition of silicon also occurs on the nanowire sidewalls, thus causing the tapering as the nanowire grows. The tapering of the nanowires can be controlled by introducing chlorinated species in the gas phase [12]. In this study, we optimized the ratio of SiH₄ and HCl flow rates to minimize the uncatalyzed silicon deposition rate, and thus the tapering. As can be seen from Fig. 3(b), single-crystalline silicon grows epitaxially on the impinging-end sidewall, presumably through pinholes in the native oxide. Lattice imaging confirmed the silicon deposit to be epitaxial and unstrained. The fringes are aligned and coherent, that is, there are no misfit dislocations, as confirmed by counting the number of $\{220\}$ lattice fringes on either side of the native oxide within a region of few tens of nanometers along the interface. Epitaxial growth of silicon was observed on the entire impinging-end sidewall, away from the area of impingement (including regions C and E). Fig. 3(c) shows a HRTEM image of the neck region (labeled as region B) that forms at the impingement location of the nanowire with the opposing sidewall. As can be seen from



the HRTEM image, no grain boundaries, abrupt interfaces, or misfit dislocations were observed in this region, which is presumably, where the actual connection is formed between the nanowire and the opposing sidewall. HRTEM imaging suggests this connection to be coherent, unstrained, and epitaxial silicon to silicon, which is a result of precise self-assembly of the nanowire after the nanowire with a molten Au–Si alloy droplet at its tip impinges on the opposing sidewall. Because the cross-section of the connection of the nanowire with the opposing sidewall was investigated, the possibility of screw dislocations cannot be ruled out.

Energy-dispersive X-ray spectroscopy (EDX) in TEM (TEM–EDX) was used to determine the location of gold catalyst that, prior to bridging, travels at the tip of the growing nanowire in the form of a molten Au–Si eutectic droplet. Fig. 4 shows the EDX spectra collected from different regions on the opposing sidewall. Within the detection limits of TEM–EDX (typically ~ 0.1 – 1.0 at%) [13], gold was not observed in regions A, B, C, E, G, and J. Gold, however, could be detected in regions D, F, and H. That is, gold was present on the surface of the neck region, as well as on the surface of the deposit significantly away from the nanowire impact area. Gold could be detected on the surface of the deposit up to about 250 nm away from the nanowire impact area, which corresponded approximately to the radius of the disc-like deposit that we reported previously [8] for the width of the trench used in the TEM investigations. The disc shape, however, is not apparent from the TEM imaging, since the $10\ \mu\text{m}$ wide trench and the deposition time used for the sample investigated allowed only limited time for catalyzed silicon deposition on the walls of the trench near the nanowire [8]. Within the detection limits of TEM–EDX, gold could not be detected

Fig. 2. (a) Bright field TEM image of a region near the base of a bridging silicon nanowire. Inset shows a convergent-beam electron diffraction (CBED) pattern taken along the $[1\bar{1}\bar{2}]$ zone axis. (b) High-resolution TEM image along a portion of a bridging silicon nanowire. The lattice fringe spacing corresponds to the d-spacing of the $\{111\}$ Si planes. The dashed line represents the edge of the nanowire.

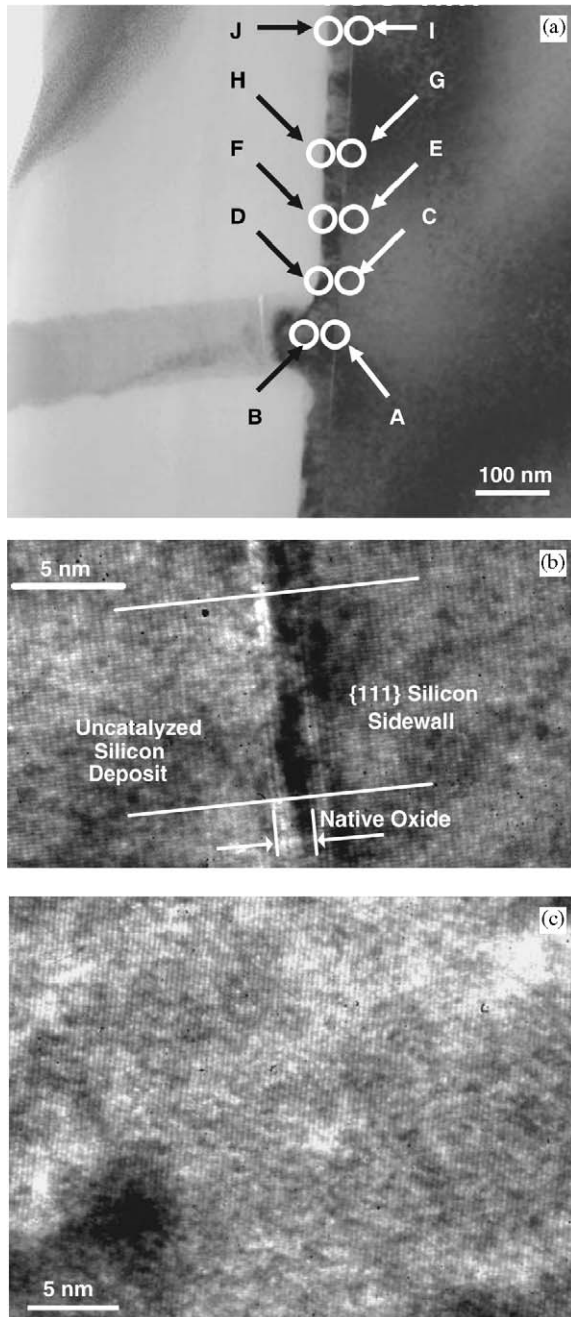


Fig. 3. (a) Low-magnification, bright-field TEM image of the impinging-end region of a bridged silicon nanowire (the different regions on the impinging-end sidewall have been labeled A through J). (b) HRTEM image of region A, the interface region of the uncatalyzed silicon deposit and the impinging-end sidewall. (c) HRTEM image of the neck region (labeled as region B in (a)) that forms at the impingement location of the nanowire with the opposing sidewall.

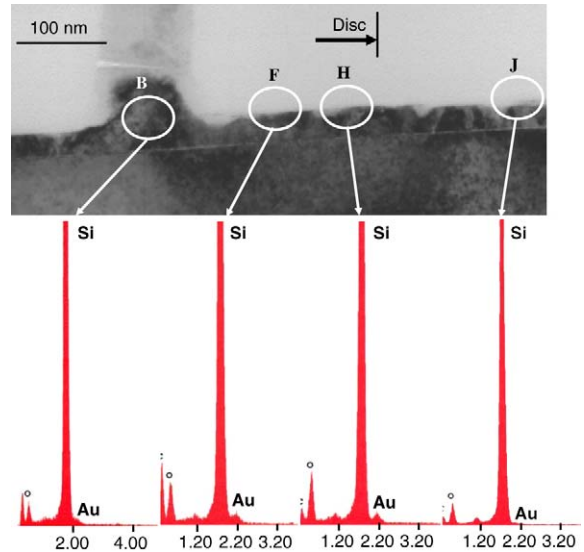


Fig. 4. EDX spectra collected from different regions on the opposing sidewall (letters correspond to positions indicated in Fig. 3.)

within the neck region or at the interface region between the opposing sidewall and the uncatalyzed silicon deposit.

Thus, HRTEM and EDX indicate that the connection of the gold-catalyzed nanowire and the opposing sidewall silicon deposit is silicon-to-silicon. We further confirmed this hypothesis by annealing the bridging nanowire samples at approximately 800 °C in hydrogen ambient, a temperature well above the Au–Si molten eutectic temperature. Upon annealing at this temperature, if there were significant gold present in the bridging region, alloying of gold and silicon would occur to form a molten eutectic, causing deformation and possibly breaking of the bridge. However, upon systematic SEM observation, we did not observe any morphological changes after annealing, again confirming the absence of significant amounts of gold within the bridging region. Our observation of the thermal stability of the self-assembled silicon-to-silicon contact is quite significant because it will allow the processing needed to integrate the bridging nanowires into electronic devices.

Based on the TEM and EDX observations, we postulate the following mechanism for the

bridging process of gold-catalyzed nanowires. The proposed mechanism is schematically depicted in Fig. 5. (1) As the gold catalyst nanoparticles selectively formed on one sidewall of a trench are

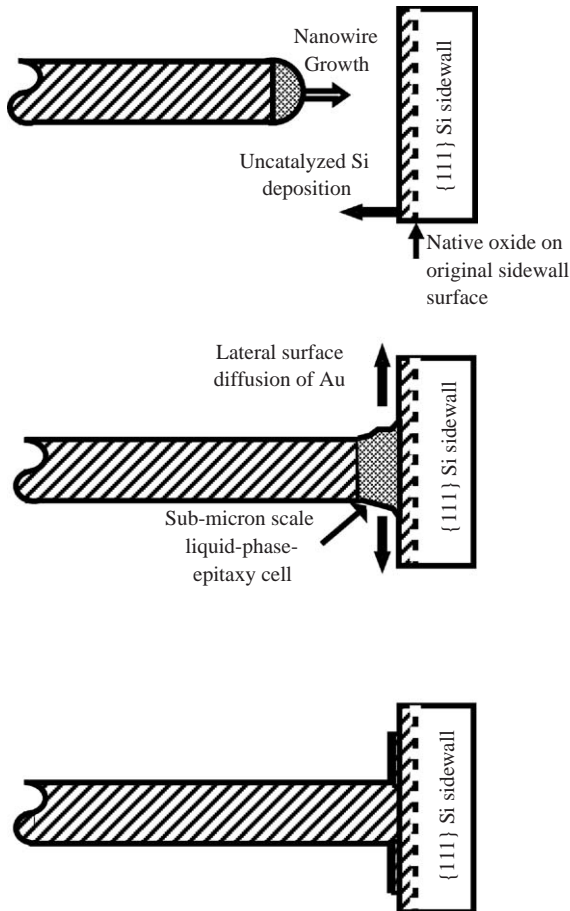


Fig. 5. Proposed mechanism for the bridging process of gold-catalyzed nanowires: As gold-catalyzed silicon nanowires start to grow, uncatalyzed, epitaxial silicon deposition also occurs through the pinholes in the native oxide on the opposing sidewall. A molten droplet of Au–Si eutectic of similar diameter as the nanowire diameter sits at the tip of the growing nanowire. As the nanowire approaches the opposing sidewall and the molten droplet makes contact with the opposing sidewall, gold-catalyzed, epitaxial silicon deposition continues on both growth surfaces (nanowire and the previously uncatalyzed Si deposit) till a firm silicon-to-silicon connection is formed. Simultaneously, the molten eutectic spreads radially outwards on the surface of the uncatalyzed silicon deposit on the opposing sidewall. The Au–Si eutectic spreading radially outwards catalyzes further silicon deposition, causing the formation of a disc-like deposit.

exposed to $\text{SiH}_4/\text{HCl}/\text{H}_2$, nanowires start to grow. Simultaneously, uncatalyzed, epitaxial silicon deposition occurs through the pinholes in the native oxide on the opposing sidewall. Nanowires grow via the conventional vapor–liquid–solid (VLS) mechanism, wherein a molten droplet of Au–Si eutectic of diameter similar to the nanowire diameter, sits at the tip of a growing nanowire. (2) As the nanowire approaches the opposing sidewall and the molten droplet makes contact with that sidewall, the molten eutectic radially spreads out from the impingement area onto the surface of the uncatalyzed silicon deposit on the opposing sidewall. The contact region of the molten eutectic and the opposing sidewall deposit constitutes a sub-micron scale liquid-phase epitaxy cell. Gold-catalyzed, epitaxial silicon deposition continues on both growth surfaces (nanowire and the previously uncatalyzed silicon deposit), till a firm and coherent silicon-to-silicon connection is formed. (3) The Au–Si eutectic spreading radially outwards along the sidewall catalyzes further silicon deposition, causing the formation of a disc-like deposit. As in the case of nanowire growth, the catalyzed deposition takes place at the interface between the liquid Au–Si eutectic and the silicon deposit on the opposing sidewall, thus causing gold to remain on the surface of the resulting deposit. The diameter of the disc-like deposit depends on the time available for molten Au–Si eutectic to spread on the surface after the impact of the nanowire with the opposing sidewall deposit. For a constant total duration of silicon deposition, the time available for Au–Si eutectic spreading after the nanowire impingement, and consequently the disc diameter, is greater for narrower trenches.

In summary, we studied the structural characteristics of bridging silicon nanowires synthesized using a gold-catalyzed chemical vapor deposition technique. Lateral silicon nanowires were grown from the vertical $\{111\}$ silicon surfaces of a trench and eventually bridged the trench. The nanowires were single crystalline, and grew along $\langle 111 \rangle$ directions. The bridging connection at the opposing sidewall was observed to be epitaxial and coherent silicon-to-silicon. Observation of such a connection formed by self-assembly is significant

for the application of the bridging nanowires in electronic devices such as sensors.

Acknowledgments

The authors thank Tan Ha of Hewlett-Packard Laboratories for expert experimental assistance. Authors also thank Ron Kelly and David Basile of HP-Corvallis for their help with the TEM sample preparation and preliminary low-magnification TEM imaging. This work was supported in part by Defense Advanced Research Projects Agency.

References

- [1] A.P. Alivisatos, *Science* 271 (1996) 933.
- [2] Y. Cui, C.M. Lieber, *Science* 291 (2001) 851.
- [3] Z. Li, Y. Chen, X. Li, T.I. Kamins, K. Nauka, R.S. Williams, *Nano Lett.* 4 (2004) 245.
- [4] T.I. Kamins, R.S. Williams, D.P. Basile, T. Hesjedal, J.S. Harris, *J. Appl. Phys.* 89 (2001) 1008.
- [5] J. Westwater, D.P. Gosain, S. Tomiya, S. Usui, H. Ruda, *J. Vac. Sci. Technol. B* 15 (1997) 554.
- [6] A.M. Morales, C.M. Lieber, *Science* 279 (1998) 208.
- [7] M.K. Sunkara, S. Sharma, R. Miranda, G. Lian, E.C. Dickey, *Appl. Phys. Lett.* 79 (2001) 1546.
- [8] M.S. Islam, S. Sharma, T.I. Kamins, R.S. Williams, *Nanotechnology* 15 (2004) L5.
- [9] M.S. Islam, S. Sharma, T.I. Kamins, R.S. Williams, *Appl. Phys. A* 80 (2005) 1133.
- [10] R.M. Langford, A.K. Petford-Long, *J. Vac. Sci. Technol. A* 19 (2001) 2186.
- [11] M.H.F. Overwijk, F.C. Van Den Heuvel, C.W.T. Bulle-Lieuwma, *J. Vac. Sci. Technol. B* 11 (1993) 2021.
- [12] S. Sharma, T.I. Kamins, R.S. Williams, *J. Crystal Growth* 267 (2004) 613.
- [13] C.E. Lyman, Physical aspects of microscopic characterization of materials, in: J. Kirschner, K. Murata, J.A. Venables (Eds.), *Scanning Microscopy International*, AMF, O'Hare, IL, 1987.